energies

MDPI

Article

Non-Vacuum Processed Polymer Composite Antireflection Coating Films for Silicon Solar Cells

Abdullah Uzum [1,2], Masashi Kuriyama [1], Hiroyuki Kanda [1], Yutaka Kimura [3], Kenji Tanimoto [3] and Seigo Ito [1,*]

1 Department of Materials and Synchrotron Radiation Engineering, Graduate School of Engineering, University of Hyogo, 2167 Shosha, Himeji, Hyogo 671-2280, Japan; auzum@ktu.edu.tr (A.U.); skyspell0922@gmail.com (M.K.); hiroyuki.k.8ch@gmail.com (H.K.)

2 Department of Electrical and Electronics Engineering, Faculty of Engineering, Karadeniz Technical University, 61080 Trabzon, Turkey

3 Specialty Materials Research Laboratory, Nissan Chemical Industries, Ltd., 11-1 Kitasode, Sodegaurashi, Chiba 299-0266, Japan; kimura@nissanchem.co.jp (Y.K.); tanimotoke@nissanchem.co.jp (K.T.)

* Correspondence: itou@eng.u-hyogo.ac.jp; Tel.: +81-79-267-4150

Academic Editor: Narottam Das

Received: 5 May 2016; Accepted: 22 July 2016; Published: 15 August 2016

Abstract: A non-vacuum processing method for preparing polymer-based ZrO_2/TiO_2 multilayer structure antireflection coating (ARC) films for crystalline silicon solar cells by spin coating is introduced. Initially, ZrO_2, TiO_2 and surface deactivated-TiO_2 (SD-TiO_2) based films were examined separately and the effect of photocatalytic properties of TiO_2 film on the reflectivity on silicon surface was investigated. Degradation of the reflectance performance with increasing reflectivity of up to 2% in the ultraviolet region was confirmed. No significant change of the reflectance was observed when utilizing SD-TiO_2 and ZrO_2 films. Average reflectance (between 300 nm–1100 nm) of the silicon surface coated with optimized polymer-based ZrO_2 single or ZrO_2/SD-TiO_2 multilayer composite films was decreased down to 6.5% and 5.5%, respectively. Improvement of photocurrent density (*Jsc*) and conversion efficiency (η) of fabricated silicon solar cells owing to the ZrO_2/SD-TiO_2 multilayer ARC could be confirmed. The photovoltaic properties of *Jsc*, the open-circuit photo voltage (V_{OC}), the fill factor (*FF*), and the η were 31.42 mA cm^{-2}, 575 mV, 71.5% and 12.91%. Efficiency of the solar cells was improved by the ZrO_2-polymer/SD-TiO_2 polymer ARC composite layer by a factor of 0.8% with an increase of *Jsc* (2.07 mA cm^{-2}) compared to those of fabricated without the ARC.

Keywords: antireflection coating; nanoparticle; spin coating; Czochralski silicon (CZ-Si); zirconium oxide (ZrO_2); titanium oxide (TiO_2); non-vacuum; low-cost solar cell

1. Introduction

Improving the absorption properties and reducing the optical losses in solar cells are crucial to achieve higher efficiencies. In conventional 100–300 μm thick crystalline silicon solar cells micrometer scale alkaline or acidic surface texturing is the primary method for trapping light in the solar cell. Additionally, various materials and thin films have been used for anti-reflection coating (ARC) purposes, including SiO_2, SiN_x, TiO_2, Al_2O_3 thin films, etc., depending to the type of solar cell. On the other hand, several nanoscale light absorption, trapping and antireflection scheme approaches including nanoscale surface texturing and nanoparticle assisted structures, and plasmonic structures has also been investigated due to their good electro-optical properties [1–3]. These approaches are based on light scattering and trapping at nanoscale approaches and mainly focus on thin film solar cells where conventional micrometer scale surface texturing is not suitable and on low grade silicon solar cells where the short carrier collection length needs to be considered. Excellent light absorption

of silicon nanostructures could be achieved by silicon nanowires [4,5], silicon pillars [6,7], silicon nanoholes [8,9] for microscale thin film solar cell applications.

Today, SiN_x films dominate in the conventional silicon solar cells industry with their effective antireflective behavior and the passivation effect which leads to high bulk lifetimes [10,11]. SiN_x or stack layers (e.g., SiN_x/SiO_x) are deposited by the well-known plasma-enhanced chemical vapor deposition (PECVD) technique [12,13]. However, the need for toxic and hazardous gases such as SiH_4 and NH_3 with vacuum processing for CVD operation and considerably high costs come along as the main drawbacks. In order to meet industrial requirements with simple low-cost technologies with high throughput, cost-effective methods need to be investigated and adapted to the solar cell manufacturing process. TiO_2 has been introduced in earlier decades as an antireflection layer for silicon solar cells [14,15], due to its good optical properties to enhance the light absorption capability because of the high refractive index of silicon solar cells. However, the photocatalytic effect on TiO_2 films whereby it can decompose organic materials under ultraviolet (UV) light [16] deteriorate the photovoltaic properties of solar-cell modules which have been made of organic polymer (ethylene-vinyl acetate: EVA). A considerable amount of literature has been published on sol-gel processes for silicon solar cells, including TiO_2, TiO_2-SiO_2 [14,15] and some Al_2O_3-based Ti doped mixed sol-gel sources have been introduced as well [17,18]. In addition to these metal oxides, ZrO_2 thin films can be another candidate as an antireflection layer with the properties of high refractive index and good thermal stability [19]. Therefore, further investigations are needed to adapt this kind of low-cost materials to the solar cell fabrication processs.

In this work, as a low temperature and non-vacuum method, spin-coating deposition was performed for polymer-metal oxide composite films. TiO_2 is a suitable material for ARC as described above. Due to the TiO_2 photocatalytic effect, however, we have confirmed the photo decomposition of the polymer-TiO_2 composite layer at the first stage, and therefore, we have utilized surface-deactivated TiO_2 nanoparticles (SD-TiO_2), afterwards. Therefore, ZrO_2-polymer (ZrO_2-P) composite films, surface-deactivated TiO_2-polymer (SD-TiO_2-P) composite films, and ZrO_2-polymer composite/surface-deactivated TiO_2-polymer (ZrO_2-P/SD-TiO_2-P) composite films were introduced as alternative anti-reflection coating films for the fabrication of silicon solar cells. The suitable order of the layers according to their refractive indexes is the key point for multilayer structure ARC films [20]. From that point of view, after confirming the structure of TiO_2 and ZrO_2 polymer-based thin films separately, an <air/ZrO_2-polymer/surface-deactivated TiO_2-polymer/Si> multilayer structure was also built considering the gradual increasing order of refractive indexes of approximately 1.5, 2, 4.3 for ZrO_2, TiO_2 and silicon, respectively, where the refractive index of air is equal to 1. Owing to the advantage of this gradual increase of refractive index on the light path, much lower reflectance can be expected [20]. After the experimental evaluations in this work, silicon solar cells were fabricated with and without using ZrO_2-P composite, ZrO_2-P/SD-TiO_2-P multilayer composite films.

2. Experimental

ZrO_2 colloidal nanoparticles (in water, ZR-30AH, Nissan Chemical Industry Co. Ltd., Chiba, Japan), surface-deactivated TiO_2 colloidal nanoparticle (in water, nanoUSE-Ti, Nissan Chemical Industry Co. Ltd.) and TiO_2 nanoparticle (in screen printing paste for dye-sensitized solar cells, PST-18NR, JGC Catalysts and Chemicals Ltd., Kanagawa, Japan) were utilized. The average diameter of particles and the rate of solid components of ZrO_2 nanoparticles, surface-deactivated TiO_2-nanoparticles and TiO_2-nanoparticles are 50 nm (30 wt %), 13 nm (30 wt %) and 18 nm (17 wt %), respectively. Transmission electron microscopy (TEM) images of each nanoparticle are given in Figure 1.

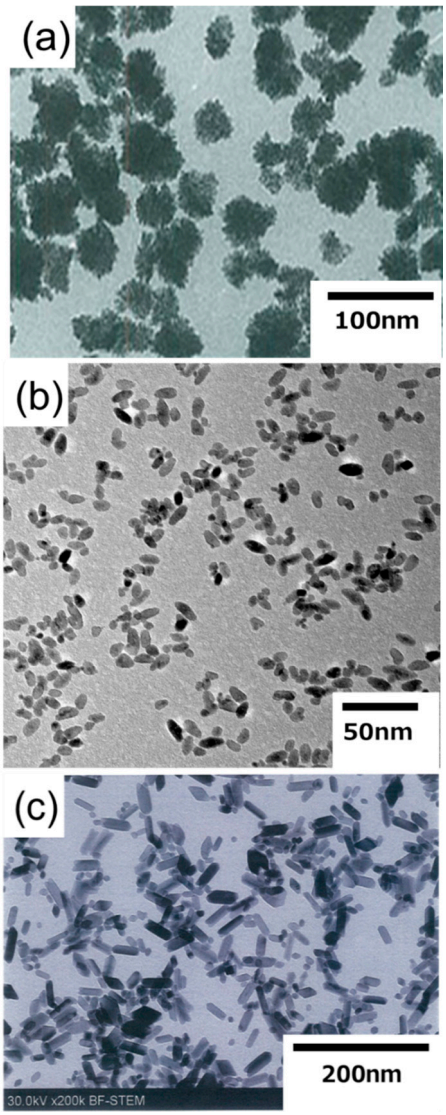

Figure 1. TEM images of nanoparticles of; (**a**) ZrO_2 (ZR-30AH, Nissan Chemical Industrial Co. Ltd., Chiba, Japan); (**b**) TiO_2 with surface deactivation (nanoUSE-TI, Nissan Chemical Industrial Co. Ltd.) and (**c**) TiO_2 (PST-18NR, JGC-CCIC Co. Ltd., Kanagawa, Japan).

Solutions for composite films were prepared by mixing one of the nanoparticles with ethanol and organic polymer (ethyl cellulose, Figure 2). The ethyl cellulose was a mixture of E0265 (9–11 mPa·s, 5% in toluene + ethanol (80:20) at 25 °C, Tokyo Chemical Industry Co., Ltd., Tokyo, Japan) and E0266 (45–55 mPa·s, 5% in toluene + ethanol (80:20) at 25 °C, Tokyo Chemical Industry Co., Ltd., Tokyo, Japan). For the mixing, 50 g of ethyl cellulose (E0265) and 50 g of ethyl cellulose (E0266) were dissolved in 1 L of ethanol, beforehand. The nanoparticle-polymer composite layers were formed on flat or alkaline textured crystalline silicon (c-Si) substrates and primary evaluation of the coating films as an antireflection coating (ARC) film.

After the initial optical analysis of TiO_2 ARC films and the confirmation of the photocatalytic effect of TiO_2, surface-deactivated TiO_2 and polymer based ZrO_2 films were evaluated as ARC. The amount of ethyl cellulose and ethanol were altered for the further analysis. Optimized solutions were named as surface-deactivated TiO_2-polymer (SD-TiO_2-P) composite films and ZrO_2-polymer (ZrO_2-P) composite films. Finally, textured p-type CZ-Si solar cells were fabricated using SD-TiO_2-P composite, ZrO_2-P composite and ZrO_2-P/SD-TiO_2-P composite multilayer structures as an ARC film on the front surface of the wafers and compared to those of solar cells without ARC.

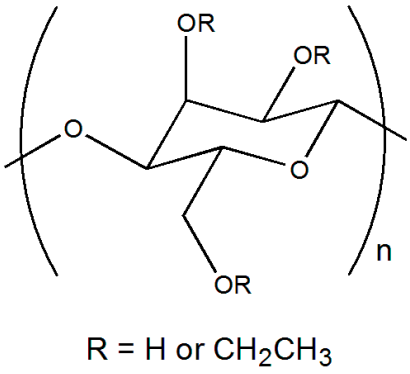

Figure 2. Structure of ethylcellulose.

For the optical measurements, square-shaped p-type Si wafers (25 × 25 mm^2) were cut out from 6-inch CZ-Si p-type wafers. All wafers were dipped into the 20% diluted HF for 1 min and rinsed in distilled water. UV/O_3 surface treatment was carried out for a complete cleaning process. All thin films in this work were coated by spin-coating method. Spin coating was carried out at 5000 rpm for 25 s (acceleration time is 5 s). All deposited films were annealed at 125 °C for 5 min. Analyses were carried out by scanning electron microscope (SEM) measurements (JSM-6510, JEOL, Tokyo, Japan), reflection analysis (by ultraviolet-visible spectroscopy, Lambda 750 UV/VIS Spectrometer, Perkin Elmer, Waltham, MA, USA) and ellipsometer (UviselErAgms-nds, Horiba Jobin Yvon, Kyoto, Japan) and finally by fabricating c-Si solar cells.

C-Si solar cells were fabricated in four different sets with a variety of surface conditions: without ARC, with SD-TiO_2-P composite, ZrO_2-P composite, or ZrO_2-P/SD-TiO_2-P composite multilayer structured ARC films. For the fabrication of c-Si solar cells, 25 × 25 mm^2 p-type CZ-Si wafers were used, which were cut out from 6-inch wafers. For surface-textured Si solar cells, alkaline texturing was performed in KOH (5.19 g) solution in H_2O (100 mL) with Alka-Tex (0.28 mL, GP Solar, Konstanz, Germany) at 80 °C (set: 100 °C) for 30 min. The silicon wafers were dipped into the 20% diluted HF for 10 min and rinsed in distilled water. Then, RCA cleaning [21,22] was carried out to remove contaminant particles on the surface of the wafers by using a $NH_4OH/H_2O_2/H_2O$ (1:1:5 in volume) solution, for 10 min at 80 °C. After removal of the natural oxide films by 20%HF, a mixed solution of $HCl/H_2O_2/H_2O$ (1:1:5 by volume) was used to remove metallic contaminants and mobile ions on the surface by dipping the wafers for 10 min at 80 °C. In order to prevent phosphorous diffusion on the back side of the silicon wafer, polysilazane was coated using spin coater by two times at 1500 rpm for 20 s, succeeded by annealing at 600 °C for 60 min in O_2 gas flow. $POCl_3$ diffusion was performed at 900 °C for 30 min with 0.2 L/min N_2 flow, in order to obtain n+ emitter. Afterwards, wafers were successively rinsed by dipping in 10% HF and pure water. Front and back contacts were formed by screen-printing Ag and Al, respectively. Co-firing was carried out at 780 °C for 1 min. SD-TiO_2-P, ZrO_2-P and ZrO_2-P/SD-TiO_2-P composite multilayer structure were deposited as ARC on the finished cells and compared to those of the cells without ARC. Deposition of ARC films were carried out after the firing step by spin coating process (5000 rpm, 5 s acceleration + 25 s) and subsequent annealing (125 °C, 5 min). For the cells with ZrO_2-P/SD-TiO_2-P composite multilayer structure ARC, first SD-TiO_2-P composite film was deposited and annealed and then ZrO_2-P composite film was deposited and annealed.

3. Results and Discussion

3.1. Evaluation of TiO_2-Polymer, Surface-Deactivated TiO_2-Polymer and ZrO_2-Polymer Composite Films

In order to observe the photocatalytic effect of TiO_2-P film when used for ARC purposes, reflectance analyses were carried out. Special attention was paid to the effect of UV light on short

wavelengths and to the long run stability analysis of the TiO_2-P film. Figure 3 shows the reflectance spectra of the silicon wafers coated with TiO_2-P, ZrO_2-P films or SD-TiO_2-P composite films on short wavelengths. Considerable differences were observed on the short wavelength between the reflectance data of each material. Reflectance was measured from 320 nm to 400 nm initially and after 8 h and 102 h from the first measurement. It was observed that the reflectance of the wafers coated with TiO_2-P coated substrate was increased in the short wavelength by the increase of the illuminating time. This increment of reflectance performance by time in shorter wavelengths can be due to the photocatalytic effect of TiO_2. This increment could be eliminated by SD-TiO_2-P in which the surface TiO_2 nanoparticles are deactivated, and then, the decomposition of organic materials under the UV light could be avoided. No significant change of the reflectance was observed on SD-TiO_2-P and ZrO_2-P coated wafers. These results are important to realize the adverse effect of photo catalysis when using TiO_2 films as an ARC. The photo catalysis effect of TiO_2 becomes rather valuable when the use of it considered for low bandgap and multi junction solar cells that the improved absorbance in UV region of the spectrum is important.

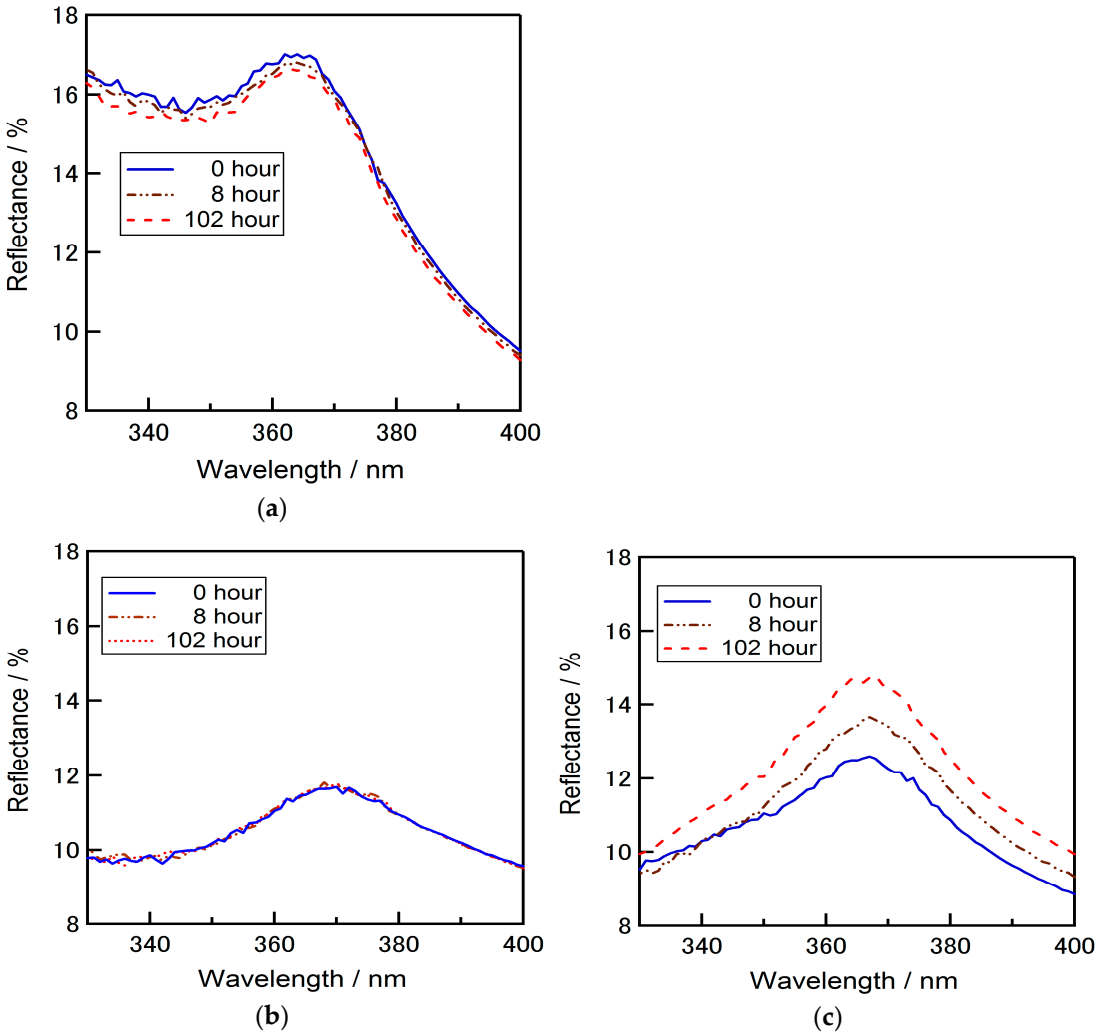

Figure 3. Stability comparison of the (**a**) ZrO_2-P; (**b**) Surface-deactivated TiO_2-P and (**c**) TiO_2-P ARC films by reflectance spectra analysis in short wavelengths.

On the other hand, the stability of a film under the continuous illumination is needed to be considered when it was aimed to be used for ARC purposes. The time dependence on the average reflectance of the TiO_2-P, ZrO_2-P and SD-TiO_2-P films on silicon substrates were carried out by

continually illuminating the films up to 102 h (under constant light illumination, 1 sun, AM 1.5). Dependence of reflectance of each ARC film to the light irradiation time is given in Figure 4 (dots show the measurement values, straight and dotted lines show the fitting for easy understanding). SD-TiO_2-P and ZrO_2-P composite films were relatively stable against light irradiation, with average reflectance of around 7% and 6.5%, respectively. However, the reflectance of TiO_2-P coated wafer increased with the irradiation time and the increase is more significant after 10 h of irradiation.

After the confirmation of the photocatalytic effect of TiO_2-P film, we focused on the SD-TiO_2-P and ZrO_2-P films as ARC layers for silicon solar cells. First, zirconium bare solution was spun on the surface of the textured wafer without any additives with spin speed of 4000 rpm for 20 s (acceleration time is 4 s).

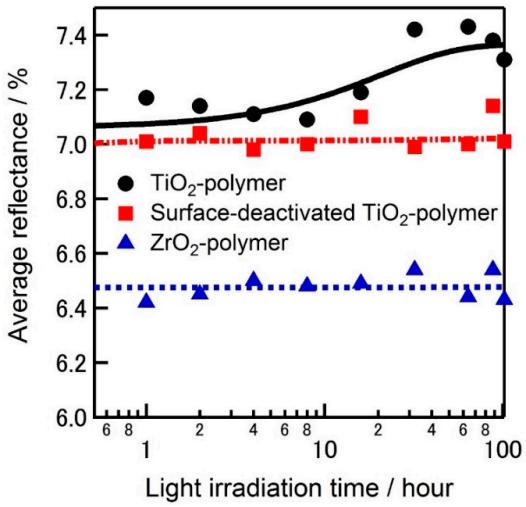

Figure 4. Time dependence of the reflectance of the silicon substrate coated with ZrO_2-P, SD-TiO_2-P and TiO_2-P ARC films.

Detrimental cracks were observed between the textured pyramids after drying, as shown in Figure 5a. To avoid these cracks, a mixed solution was prepared with ethanol (1:1 in volume). However, cracks were could not be avoided totally.

In order to achieve a smooth surface without any cracks, ethyl cellulose was added into the bare zirconium solution. Ethyl cellulose is a non-toxic polymer with good mechanical, physical and chemical properties, including high flexibility, high resistance to moisture and excellent elasticity, which makes it a quality film former [23]. Moreover, it dissolves in a wide range of solvents and alcohols, which is important for our solution that contains ethanol [23]. The ratio of ethyl cellulose solution, ethanol and zirconium solution was 1:32:2 (by volume). Spin coating of the latter solution was carried out with similar parameters. Crack-free and smooth surface could be confirmed as shown in Figure 5b (this is the final solution for ZrO_2-P composite film that is used in subsequent experiments). Eliminating the cracks can be attributed to the flexibility and the strength added by ethyl cellulose in the solution. It is also worth mentioning that the good light permeability of the ethyl cellulose makes it an appropriate material to utilize such a solution aimed to be used for ARC material where the transparency is so important. Similarly, surface-deactivated TiO_2 solution was spun on the surface of the textured wafer with a various composition of TiO_2 solution and ethanol and surface condition of the wafers was examined. 1 mL TiO_2 solution mixed with 2, 4, 6 or 8 mL ethanol and spun on the textured silicon wafer with spin speed of 5000 rpm for 25 s (acceleration time is 5 s), as shown in Figure 6a–d. Cracks were observed between the pyramids when the TiO_2 solution was mixed with 2, 4 or 6 mL of ethanol. Surface condition and cracks can be confirmed in the corresponding enlarged images embedded in Figure 6a–c. Fortunately, TiO_2 solution mixed with 8 mL of ethanol combination provided crack-free surface.

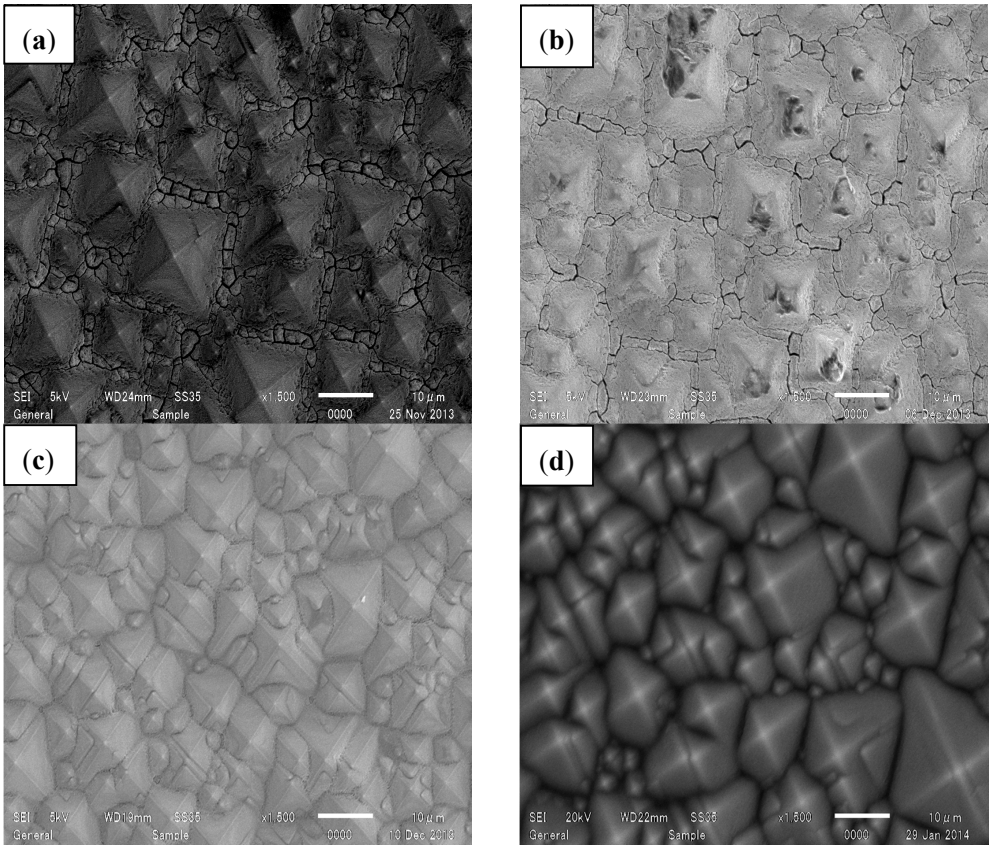

Figure 5. SEM surface images of antireflection coating by ZrO_2 sol on textured Si surface; (**a**) pure ZrO_2 sol; (**b**) ZrO_2 sol (1 mL) + ethanol (1 mL); (**c**) ZrO_2 sol (1 mL) + ethanol (9 mL); (**d**) ZrO_2 sol (0.5 mL) + ethanol (8 mL) + 10% ethyl cellulose solution in ethanol (0.25 mL).

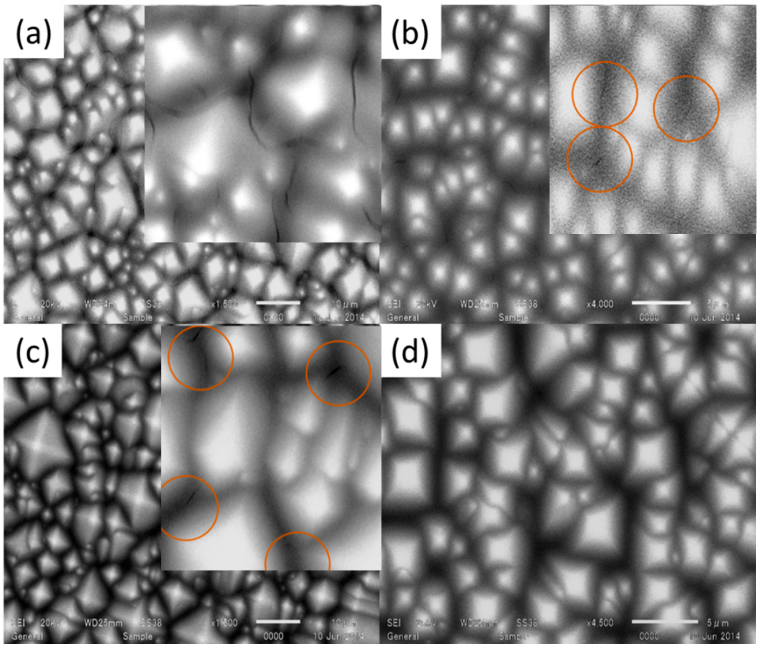

Figure 6. SEM surface images of antireflection coating by surface-deactivated TiO_2 sol on Si surface; (**a**) 2 mL ethanol + 1 mL TiO_2 sol; (**b**) 4 mL ethanol + 1 mL TiO_2 sol; (**c**) 6 mL ethanol + 1 mL TiO_2 sol; (**d**) 8 mL ethanol + 1 mL TiO_2 sol. The circles indicate the position of cracks.

For the initial evaluations of the ZrO_2-P films, it was deposited on flat silicon substrate by a spin-on coating method with a spin-speed in a range from 1000 to 4000 rpm for 20 s (acceleration time is 4 s). Figure 7a compares the reflectivity of flat silicon substrates w/ and w/o ZrO_2-P layer coated on the surface. The lowest average reflectance (the reflectance average between the wavelength of 300 nm–1100 nm) of 28% was achieved by ZrO_2 coating with a spin speed of 1000 rpm (Figure 7b), a steady reflectance tendency from wavelength of around 700 to 1000 nm can also be confirmed. Comparing these results it can be confirmed that the average reflectance of a silicon substrate decreased from 40% down to 28% owing to the formed ZrO_2 film on the flat silicon surface.

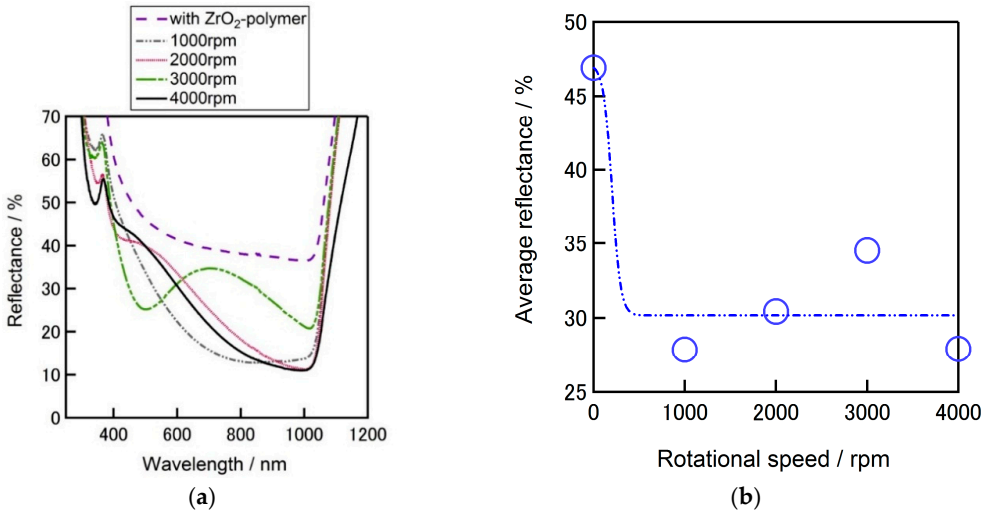

Figure 7. Reflectance spectra of flat surface silicon substrate with ZrO_2-polymer composite ARC; (**a**) by changing the spin-coat rotating speed; (**b**) the average reflectance.

Figure 8a shows the comparison of the reflectivity of textured silicon wafers covered by ZrO_2-P composite film including different amount of ethanol in the solution. Average reflectance was decreased from 8% down to 6.5%, when 8 mL (91.4%vl) ethanol is used in total zirconium solution (0.5 mL zirconium solution (5.71%vl) + 0.25 mL ethyl cellulose (2.85%vl)). Figure 8b clearly shows that there is a breaking point for the amount of ethanol used in zirconium solution to achieve better reflectance performance which is the main agent to adjust the viscosity.

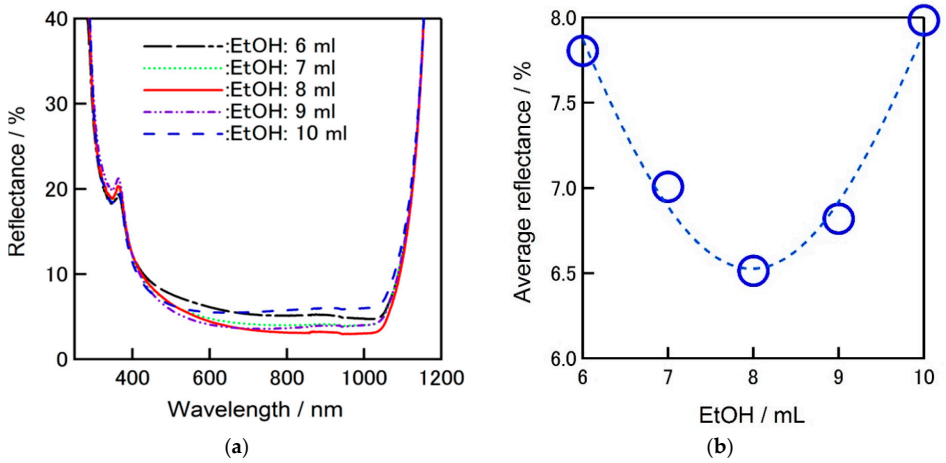

Figure 8. The comparison of the reflectance of textured silicon surface covered by ZrO_2-polymer composite film including different amount of ethanol in the solution; (**a**) reflectivity dependence on wavelength; (**b**) comparison of average reflectance dependent to the amount of ethanol in the solution.

Reflectance dependence of ZrO_2-P composite film coated alkaline textured silicon substrates on the applied spin speed is given in Figure 9a. Deposition was performed by spin-on coating with a spin-speed in a range of 500–3000 rpm. A gradual decrease of reflectance was observed with increase of spin speed and becomes relatively stable after 1500 rpm. Average reflectance of lower than 7% was confirmed when the spin speeds is 1500 rpm. The dependence of reflectance to the spin speed is given in Figure 9b. These results further support the benefit of ZrO_2-P composite film on decreasing the reflectance when formed on a silicon substrate.

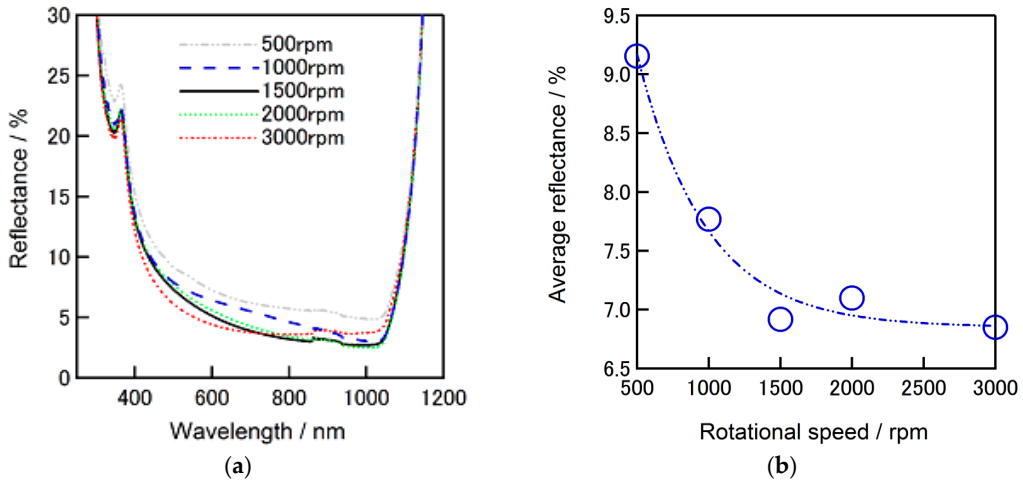

Figure 9. Reflectance of texture surface silicon substrate with ZrO_2-polymer composite ARC; (**a**) by changing the spin-coat rotating speed and (**b**) the average reflectance.

Evaluations of SD-TiO_2 solution were also carried out both on flat or textured silicon substrate. In 1 mL SD-TiO_2 solution, 0.1 mL of ethyl cellulose was added and the amount of ethanol was varied from 4 to 10 mL. Prepared solution was spun on flat silicon surface and annealed on a hot plate at 125 °C for 5 min. Figure 10 shows the reflectivity of flat silicon surface coated with TiO_2 solution with varied amount of ethanol in precursor, with spin speed of 5000 rpm or 8000 rpm. In Table 1, the average reflectance of flat silicon surface coated with surface deactivated TiO_2-ethyl cellulose film is summarized for each amount of ethanol in the solution.

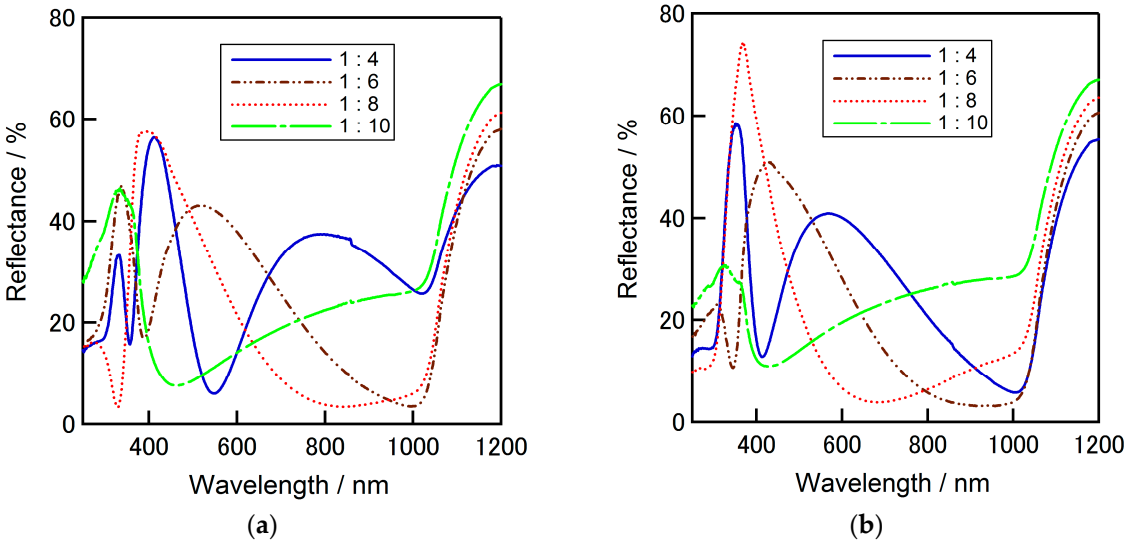

Figure 10. Reflectivity of flat silicon surface with surface-deactivated TiO_2-polymer composite ARC; (**a**) 5000 rpm (**b**) 8000 rpm. The inset shows the volume ratio of <surface-deactivated TiO_2–sol: ethanol>.

Table 1. Average reflectance of flat silicon surface with surface-deactivated TiO_2-polymer ARC coating by different spin-coating speeds. The volume of surface-deactivated TiO_2–sol was 1 mL.

Speeds \ EtOH (mL)	4	6	8	10
5000 rpm	30.00	24.00	19.92	22.66
8000 rpm	25.78	20.83	20.04	24.15

The lowest average reflectance was observed when the amount of ethanol is 8 mL, as of 19.92% and 20.04% for spin speed of 5000 rpm and 8000 rpm, respectively. Figure 11a presents the reflectivity of textured silicon surface coated with SD-TiO_2-P film. The amount of ethanol was varied similarly from 4 to 10 mL. From the figure it can be confirmed that the coated film with the precursor include 8 mL of ethanol provides the lowest reflectance. The average reflectance tendency depends on the ethanol amount can be seen in Figure 11b where the lowest average reflectance is around 5.6%.

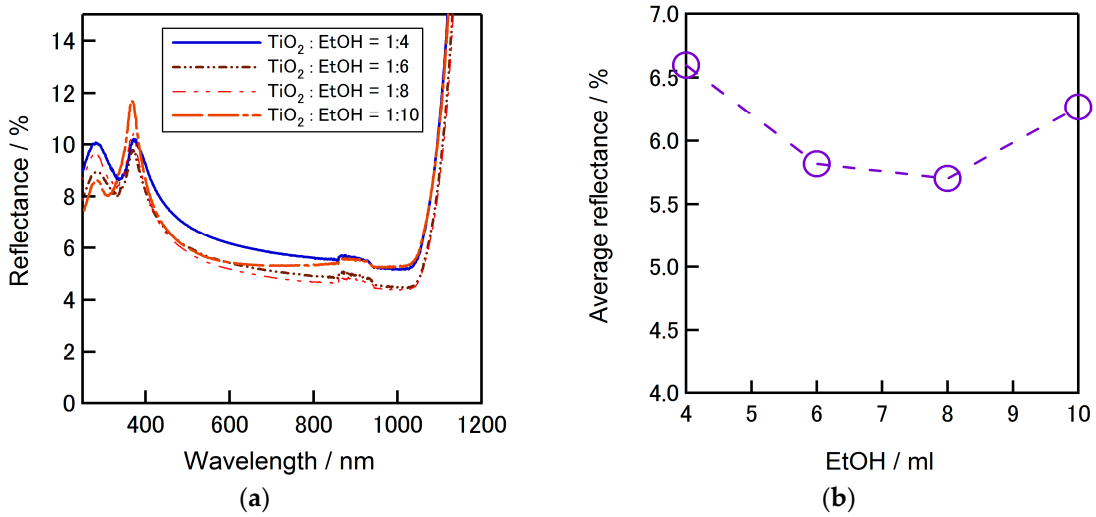

Figure 11. (**a**) Reflectance spectra of textured silicon surface with surface-deactivated TiO_2-polymer antireflection coating; and (**b**) the average reflectance from 300 nm to 1100 nm.

3.2. Simulation and Formation of ZrO_2-Polymer/Surface-Passivated TiO_2-Polymer Composite Multilayer Film

After evaluating the ZrO_2-P and SD-TiO_2-P composite thin films separately, an <air/ZrO_2-polymer/surface-passivated TiO_2-polymer/Si> multilayer structure was also built considering that the reflectance can be reduced significantly with multilayer films [20] where the layers should be deposited with gradual increase order of their refractive indexes, as $n_{air} < n_{ZrO2\text{-}polymer} < n_{TiO2\text{-}polymer} < n_{silicon}$, in this work. The refractive indexes and extinction coefficients of ZrO_2-P and SD-TiO_2-P composite layers achieved by fitting of the ellipsometry measurements are shown in Figure 12a,b, respectively. As such, refractive indexes of air and silicon wafer are 1 and 4.3, respectively.

A simulation study was carried out for the <air/ZrO_2-polymer (ZrO_2-P)/surface-deactivated TiO_2-polymer (SD-TiO_2-P)/Si> structure in order to estimate the short circuit current density (*Jsc*) density. Fresnel equations were followed by considering the measured refractive indexes of each layer in order to achieve an ideal reflectance of the total structure [24]. Fresnel approach reduces multi number of layer structure to a single imaginary layer by taking account the refractive index and thickness of each layer in the multi structure and is based on the transmittance and the reflectance waves from the corresponding layers.

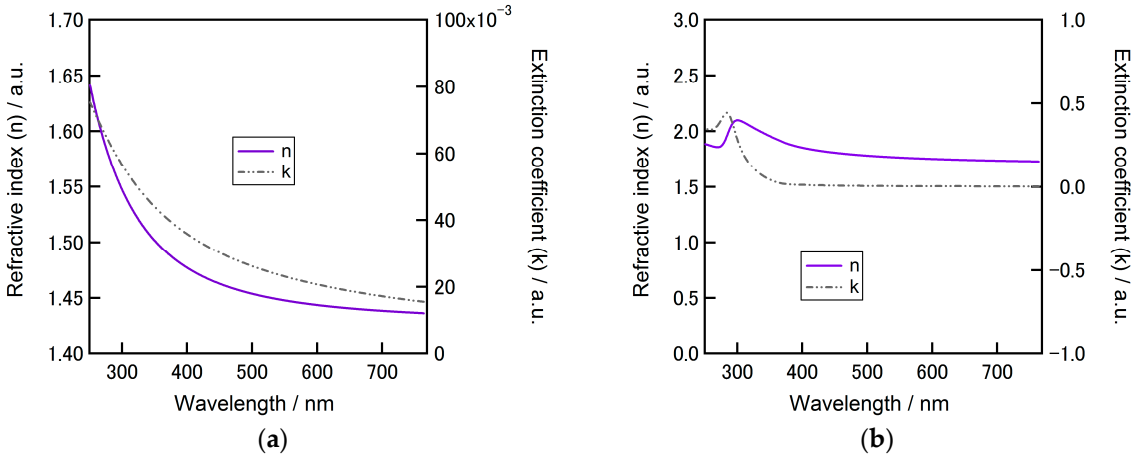

Figure 12. Fitting of ellipsometry measurements of; (**a**) nano-colloid ZrO_2 (ZR30-AH)-polymer composite; and (**b**) surface-deactivated TiO_2-polymer composite.

The thicknesses of the ZrO_2-P and SD-TiO_2-P composite layers were varied from 10 to 100 nm, and "Incident Photon to Current Conversion Efficiency (IPCE)" was assumed 100% for the calculation. *Jsc* was calculated using the Equation (1) in order to observe the ideal ZrO_2-P and SD-TiO_2-P composite film thicknesses to obtain an efficient ZrO_2-P/SD-TiO_2-P composite multilayer ARC film:

$$J_{sc,max} \leq \frac{eS}{hc} \int_{300}^{1200} P_{in} \times Abs\,(\lambda)\ d\lambda \quad (1)$$

where "*Jsc,max*" is maximum short circuit current density in mA cm^{-2}, "e" is stands for charge of an electron (1.602×10^{-19} C), "h" is Plank's constant (6.626×10^{-34} Js), "c" is speed of light (2.998×108 m·s^{-1}), "Pin" is the incident power in W/m^2, and "λ" is the wavelength in nm.

Figure 13 presents the estimated *Jsc* with ZrO_2-P/SD-TiO_2-P composite ARC film on c-Si solar cells. A summary of the estimated values of *Jsc* can be seen in Table 2 for each thickness combination of the layers.

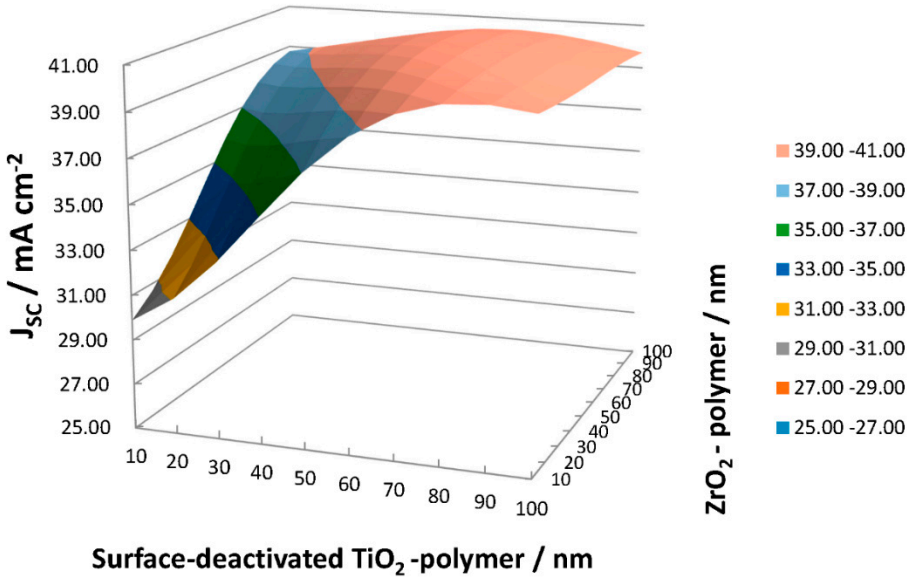

Figure 13. Simulated photocurrent density with variations of ZrO_2-polymer and surface-deactivated TiO_2-polymer thicknesses on flat-surface silicon solar cells.

Table 2. Simulated data of photocurrent density with variations of ZrO_2-polymer composite and surface-deactivated TiO_2-polymer composite thickness on flat-surface silicon solar cells.

ZrO_2/nm \ TiO_2/nm	10	20	30	40	50	60	70	80	90	100
10	29.90	31.07	32.82	34.95	37.02	38.65	39.72	40.27	40.37	40.15
20	30.66	32.12	34.07	36.18	38.03	39.36	40.15	40.46	40.39	40.06
30	31.74	33.42	35.40	37.33	38.88	39.92	40.46	40.58	40.38	39.98
40	33.06	34.81	36.66	38.31	39.55	40.33	40.66	40.65	40.37	39.94
50	34.48	36.13	37.73	39.07	40.03	40.59	40.78	40.68	40.37	39.93
60	35.84	37.27	38.56	39.60	40.33	40.73	40.83	40.69	40.36	39.93
70	37.00	38.13	39.13	39.92	40.47	40.76	40.82	40.66	40.35	39.92
80	37.87	38.72	39.45	40.04	40.47	40.71	40.76	40.60	40.30	39.89
90	38.45	39.04	39.56	40.01	40.37	40.60	40.64	40.50	40.21	39.82
100	38.76	39.13	39.50	39.87	40.20	40.43	40.47	40.35	40.08	39.72

Maximum J_{SC} of 40.83 mA cm^{-2} was achieved with <t = 60 nm ZrO_2-P/t = 70 nm SD-TiO_2-P> multilayer ARC film. It is notable that increased values of *Jsc* of ~40 mA cm^{-2} become achievable with the thickness of >50 nm of each layer.

To form and characterize such a multilayer film experimentally, first SD-TiO_2-P film was spin coated on the textured silicon surface and annealed at 125 °C for 5 min, then the reflectance of the surface was measured. After the measurement ZrO_2-P film was spin coated on SD-TiO_2-P film and annealed similarly. The comparison of reflectance spectra of textured silicon surface coated with SD-TiO_2-P film or the ZrO_2-P/SD-TiO_2-P composite multilayer film is given in Figure 14. Average reflectance of the silicon surface was improved due to the multilayer ARC where the average reflectance is around 5.5% for multilayer structure (average reflectance without ARC = 16.3%).

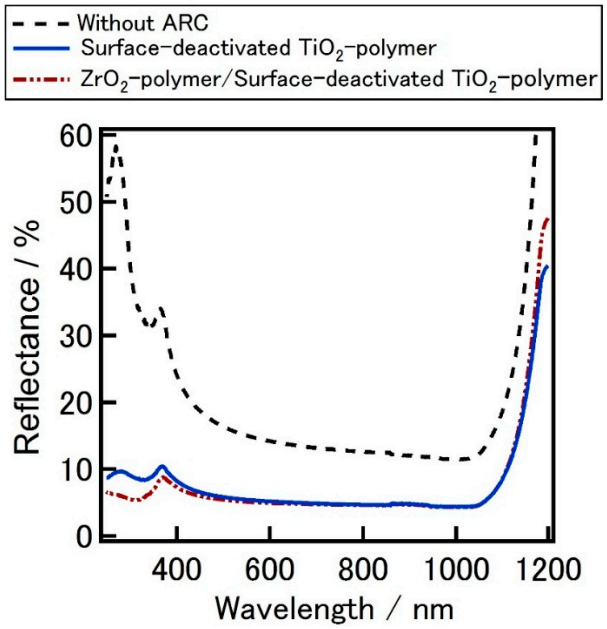

Figure 14. Reflectance spectra of textured silicon surface without ARC, with surface-deactivated TiO_2-polymer, ZrO_2-polymer/surface-deactivated TiO_2-polymer multilayer ARC.

Additionally, lifetime analysis was carried out in order to estimate the passivation effect of purposed ARC films. Four sets of samples (three samples per set) were prepared for lifetime studies; TiO_2-P (set 1), ZrO_2-P (set 2), SP-TiO_2-P (set 3), ZrO_2-P/SP-TiO_2-P (set 4). All samples went through an acidic etching of HF:HNO_3 (1:5vl%) for 5 min and then received UV/O_3 treatment for 15 min before

the film deposition. ARC films were spin coated on both sides of the wafers at 5000 rpm for 25 s (acceleration time is 5 s) and were annealed at 125 °C for 5 min.

Lifetime measurements were carried out by microwave photoconductive decay (μ-PCD) technique. Bulk lifetime of a reference sample was measured using chemical passivation (ethanol:iodine, 0.025 M) and measured as 527 μs. Samples of each set (neighbor samples cut from the same large area CZ p-type silicon wafer) were measured before (without ARC) and after forming the ARC film. Measured lifetimes are shown in Table 3. Although a slight increase of lifetimes was observed stable for those of the wafers coated with TiO_2-P or ZrO_2-P/SP-TiO_2-P multilayer ARC, however the increase was negligibly small. The maximum lifetime increases of around 0.9 μs were observed on ZrO_2-P/SP-TiO_2-P multilayer ARC coated wafers. These results show that there is no significant passivation effect of our ARC films.

Table 3. Lifetimes of the wafers measured before and after forming TiO_2-P, ZrO_2-P, SP-TiO_2-P, ZrO_2-P/SP-TiO_2-P ARC films.

	Sample No.	Lifetime/μs (before ARC)	Lifetime/μs (after ARC)	Increment/μs
TiO_2-P	1	10.35	10.88	0.53
	2	10.29	10.72	0.43
	3	10.22	10.75	0.53
ZrO_2-P	1	10.26	10.02	−0.24
	2	10.1	10.28	0.18
	3	10.22	10.56	0.34
SP-TiO_2-P	1	10.22	10.21	−0.01
	2	10.2	10.45	0.25
	3	11.2	11.6	0.4
ZrO_2-P/SP-TiO_2-P	1	11.06	11.9	0.84
	2	11.22	12.11	0.89
	3	11	11.55	0.55

3.3. Evaluation of the Fabricated p-type Crystalline Silicon Solar Cells

After the evaluation of the ARC films, CZ-Si p-type solar cells were fabricated by applying ZrO_2-P, SD-TiO_2-P composite films and ZrO_2-P/SD-TiO_2-P composite multilayer structure films as ARC layer and compared with those of the cells fabricated without any ARC film. The electrical characteristics of the fabricated solar cells with (w/) or without (w/o) ZrO_2-P composite ARC are summarized in Table 4.

Table 4. Photovoltaic characteristic of fabricated silicon solar cells on flat or textured silicon surface, w/ or w/o ZrO_2-polymer ARC.

ARC	Surface Structure	*Jsc*/mA cm^{-2}	*Voc*/V	*FF*/%	η/%
w/o ARC	flat	24.03	0.527	57.1	7.25
w/ ZrO_2-polymer composite	flat	30.22	0.537	60.2	9.78
w/o ARC	textured	28.74	0.511	69.4	10.20
w/ ZrO_2-polymer composite	textured	30.62	0.510	69.7	10.89

Conversion efficiency of the best cell fabricated on flat silicon substrate w/o ZrO_2-P composite ARC on the surface was 7.25% with *Jsc* and open circuit voltage (*Voc*) of 24.03 mA cm^{-2}, 527 mV, respectively. Conversion efficiency of the cell w/ ZrO_2-P composite ARC, reaches 9.78% with *Jsc* of 30.22 mA cm^{-2}, owing to the light trapping by ZrO_2-P composite ARC film. *Jsc* of the solar cells fabricated on textured silicon substrates increase up to 29.74 mA cm^{-2} (w/o ZrO_2-P ARC) and 30.62 mA cm^{-2} (w/ ZrO_2-P ARC) due to reduced reflection by textured surface and ZrO_2-P composite ARC film. Conversion efficiencies of the solar cells with textured surface were 10.2% and 10.9 for those

cells w/ and w/o ZrO_2-P ARC, respectively. Figure 15 presents the *J-V* curve comparison of the best cells for each set.

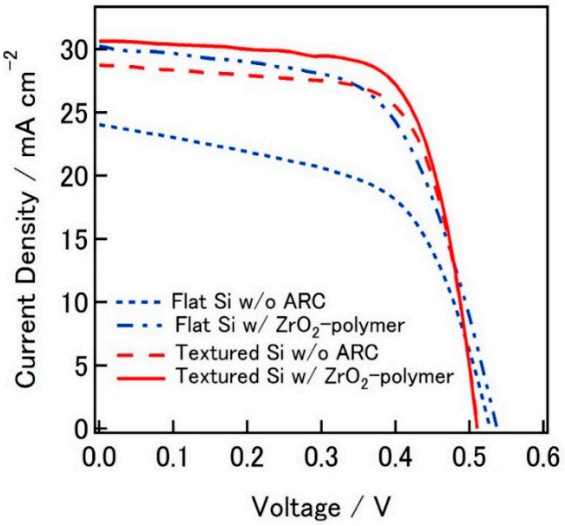

Figure 15. *J-V* curves of flat-surface or textured-surface silicon solar cells w/ or w/o ZrO_2-polymer composite ARC film.

On the other hand, solar cells with SD-TiO_2-P ARC and ZrO_2-P/SD-TiO_2-P composite multilayer ARC were also fabricated. *Jsc* of 30.93 mA cm^{-2} and *Voc* of 569 mV were achieved when solar cells fabricated w/o any ARC (average of three samples). Average *Jsc* of the solar cell with SD-TiO_2-P composite film and ZrO_2-P/SD-TiO_2-P composite multilayer film as ARC increased up to 32.44 and 33.00 mA cm^{-2}, respectively. These increases of *Jsc* are attributed to the decrease of the reflectance with ARCs which increases the optical performance of the solar cells. Average efficiencies of the three fabricated cells for each set, w/o ARC, w/ SD-TiO_2-P film and w/ ZrO_2-P/SD-TiO_2-P composite multilayer structure film were 11.99%, 12.84%, and 12.85%, respectively. Table 5 summarizes the electrical characteristics of the fabricated solar cells. Efficiency of the solar cells improved by a factor of 0.86% with an increase of *Jsc* (2.07 mA cm^{-2}) by the contribution of ZrO_2-P/SD-TiO_2-P ARC composite multilayer compared to those of fabricated without the ARC. The best efficiency of 12.91% for the cells with ZrO_2-P/SD-TiO_2-P composite multilayer structure ARC film was achieved with *Jsc* of 31.42 mA cm^{-2}, *Voc* of 575 mV, and fill factor (*FF*) of 71.5%. The *J-V* curve comparison of the best cells for each set is given in Figure 16. The higher average *Jsc* of the cells than that of the best cells in spite of lower *FF* may draw the attention which can be attributed to the ARC effect. Because the lower series resistances of the best cells might be due to the lower contact resistance owing to the better contact formation between the metal contacts and silicon during the firing steps which lead higher *FF*.

Table 5. Best and average cell data of photovoltaic characteristics for fabricated silicon solar cells without ARC and with surface-deactivated TiO_2-polymer or ZrO_2-polymer/Surface-deactivated TiO_2 polymer composite ARC films. Average data for each set is for three different samples.

Structure of Solar Cells		*Jsc*/mA cm^{-2}	*Voc*/V	*FF*/%	*Rseries*/Ω·cm^2	*Rshunt*/Ω·cm^2	η/%
Without ARC	**Best**	**29.33**	**0.570**	**71.7**	**0.73**	**782**	**11.99**
	Average	30.93	0.569	63.1	1.23	406	11.06
Surface-deactivated TiO_2 polymer	**Best**	**30.90**	**0.574**	**72.3**	**0.66**	**548**	**12.84**
	Average	32.44	0.575	63.7	1.18	321	11.84
ZrO_2-polymer/Surface-deactivated TiO_2 polymer	**Best**	**31.42**	**0.575**	**71.5**	**0.75**	**504**	**12.91**
	Average	33.00	0.574	62.7	1.32	309	11.85

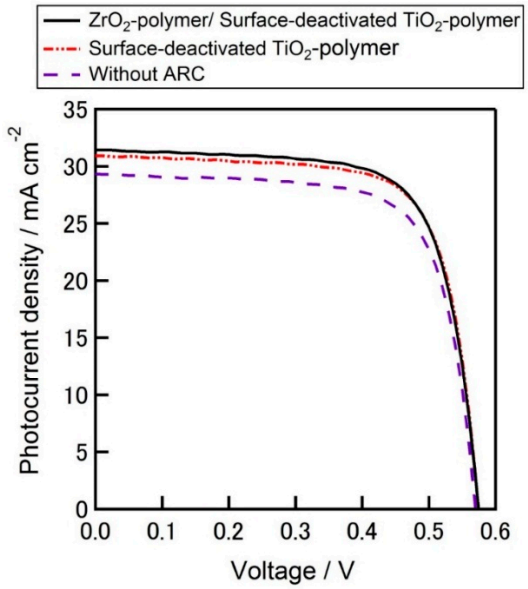

Figure 16. *J-V* curve of the best fabricated solar cells without any ARC film and with surface-deactivated TiO_2-polymer composite or ZrO_2-polymer composite/Surface-deactivated TiO_2 polymer-composite multilayer structure ARC films.

The improvement of *Jsc* by SD-TiO_2-P or ZrO_2-P/SD-TiO_2-P multilayer ARC composite can be clearly seen in Figure 17, where the *Jsc* increases gradually for all samples by SD-TiO_2-P single layer ARC and ZrO_2-P/SD-TiO_2-P multilayer ARC composite. *Jsc* increases (average of four samples) from 30.04 to up to 32.07 mA cm^{-2}. In order to discuss the statistical errors about the resulting silicon solar cells, the number of samples was not enough because just four cells have been fabricated for Figure 17. However, every cell improved the *Jsc* with sequential addition of the TiO_2-P and ZrO_2-P composite coating on the silicon surface. Hence, it was enough to understand the merit for the polymer composite layers to be the antireflection coatings.

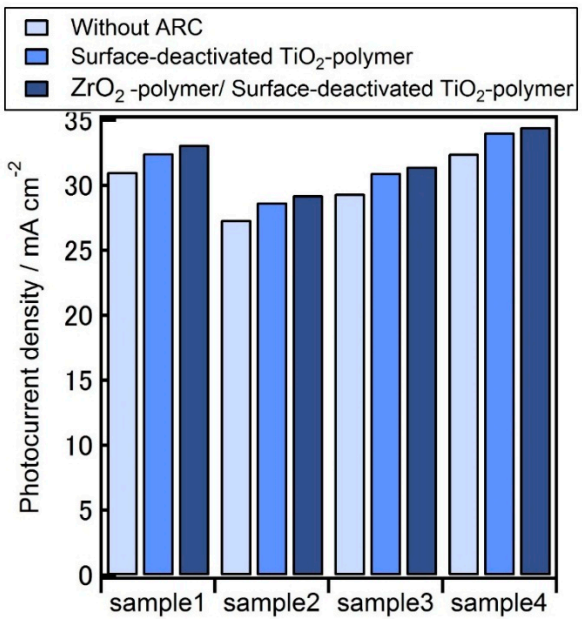

Figure 17. Comparison of photo current density for SD-TiO_2-P single layer and ZrO_2-P/SD-TiO_2-P multilayer ARC.

It should be noted that the limited overall cell performance in this work, compared to commercially available, fully state-of-art solar cells can be mainly attributed to the low lifetime of silicon substrates and inadequate bulk passivation which can cause poor *Voc* and to the low *FF* s which can be due to the lack of proper edge isolation of the finished cells. These results suggest that ZrO_2-P/SD-TiO_2-P composite multilayer structure ARC film formed by spin coating deposition technique could be beneficial and promising alternative as a low-cost, simple and vacuum-less process for ARC for silicon solar cells. Further investigations are on progress to achieve better performances on ARC utilizing polymer based ZrO_2 composite layers and its multilayer structures.

4. Conclusions

ZrO_2-polymer composite/surface-deactivated TiO_2-polymer composite films were prepared by a low-cost spin coating deposition method as an alternative ARC film for c-Si solar cells. The deteriorative effect of the photocatalytic properties of TiO_2 on reflectance performance of silicon wafers coated with TiO_2-polymer composite film was confirmed. No degradation was observed on ZrO_2-polymer composite film and surface-deactivated TiO_2-polymer composite films coated wafers for the same UV region. Good quality of ZrO_2/TiO_2 based multilayer thin films was observed for films formed at a very low temperature of 125 °C. After the evaluation of thin films, CZ-Si p-type solar cells were fabricated w/ and w/o ARC. The best efficiency of 12.91% for the cells with ZrO_2-polymer composite/surface-deactivated TiO_2 polymer multilayer structure composite ARC film was achieved with *Jsc* of 31.42 mA cm^{-2}, *Voc* of 575 mV, and fill factor *(FF)* of 71.5%. Efficiency of the solar cells improved by a factor of 0.86% with an increase of *Jsc* (2.07 mA cm^{-2}) owing to the ZrO_2-polymer/surface-deactivated TiO_2 polymer composite ARC layer compared to those of fabricated without the ARC. Considering the non-vacuum process and simplicity, polymer-based ZrO_2/TiO_2 ARC films produced by the spin coating deposition method were found to be very attractive and promising for c-Si solar cells with good optical performance which can be improved by further optimizations and investigations.

Author Contributions: Abdullah Uzum supervised the research and drafted the manuscript. Masashi Kuriyama and Hiroyuki Kanda performed the device fabrication in this study. Abdullah Uzum, Masashi Kuriyama, Hiroyuki Kanda, Seigo Ito analyzed the data. Yutaka Kimura and Kenji Tanimoto provided ZrO_2 and TiO_2 nanocolloids. Seigo Ito supervised the research, organized the laboratory for this work and finalized the manuscript.

Conflicts of Interest: The authors declare no conflict of interest.

Abbreviations

The following abbreviations are used in this manuscript:

ARC	Antireflection coating
SD-TiO_2-P	Surface deactivated-TiO_2 polymer
TiO_2-P	TiO_2 polymer
ZrO_2-P	ZrO_2 polymer
PECVD	Plasma-enhanced chemical vapor deposition
w/	with
w/o	without
vl	volume
c-Si	Crystalline silicon
UV	Ultra-violet
SEM	Scanning electron microscope
TEM	Transmission electron microscopy
μ-PCD	Microwave photoconductive decay
FF	Fill factor

References

1. Li, J.; Yu, H.; Li, Y.; Wang, F.; Yang, M.; Wong, S.M. Low aspect-ratio hemispherical nanopit surface texturing for enhancing light absorption in crystalline Si thin film-based solar cells. *Appl. Phys. Lett.* **2011**, *98*, 021905. [CrossRef]
2. Pudasaini, P.R.; Ayon, A.A. Nanostructured thin film silicon solar cells efficiency improvement using gold nanoparticles. *Phys. Status Solidi A* **2012**, *209*, 1475–1480. [CrossRef]
3. Pudasaini, P.R.; Ayon, A.A. Nanostructured plasmonics silicon solar cells. *Microelectron. Eng.* **2013**, *110*, 126–131. [CrossRef]
4. Garnett, E.; Yang, P. Light trapping in silicon nanowire solar cells. *Nano Lett.* **2010**, *10*, 1082–1087. [CrossRef] [PubMed]
5. Lin, C.; Povinelli, M.L. The effect of plasmonic particles on solar absorption in vertically aligned silicon nanowire arrays. *Appl. Phys. Lett.* **2010**, *97*, 071110. [CrossRef]
6. Pudasaini, P.R.; Elam, D.; Ayon, A.A. Aluminum oxide passivated radial junction sub-micrometre pillar array textured silicon solar cells. *J. Phys. D Appl. Phys.* **2013**, *46*, 235104. [CrossRef]
7. Li, J.; Yu, H.; Wong, S.M.; Zhang, G.; Sun, X.; Lo, P.G.-Q.; Kwong, D.-L. Si nanopillar array optimization on Si thin films for solar energy harvesting. *Appl. Phys. Lett.* **2009**, *95*, 033102. [CrossRef]
8. Han, S.E.; Chen, G. Optical absorption enhancement in silicon nanohole arrays for solar photovoltaics. *Nano Lett.* **2010**, *10*, 1012–1015. [CrossRef] [PubMed]
9. Peng, K.-Q.; Wang, X.; Li, L.; Wu, X.-L.; Lee, S.-T. High-Performance silicon nanohole solar cells. *J. Am. Chem. Soc.* **2010**, *132*, 6872–6873. [CrossRef] [PubMed]
10. Richards, B.S. Comparison of TiO_2 and other dielectric coatings for buried-contact solar cells: A review. *Progress Photovolt. Res. Appl.* **2004**, *12*, 253–281. [CrossRef]
11. Dekkers, H.F.; Beaucarne, G.; Hiller, M.; Charifi, H.; Slaoui, A. Molecular hydrogen formation in hydrogenated silicon nitride. *Appl. Phys. Lett. AIP* **2006**, *89*, 211914. [CrossRef]
12. Aberle, A.; Hezel, R. Progress in low-temperature surface passivation of silicon solar cells using remote-plasma silicon nitride. *Progress Photovolt.* **1997**, *5*, 29–50. [CrossRef]
13. Wan, Y.; McIntosh, K.R.; Thomson, A.F. Characterisation and optimisation of PECVD SiNx as an antireflection coating and passivation layer for silicon solar cells. *AIP Adv.* **2013**, *3*, 032113. [CrossRef]
14. Brinker, C.J.; Harrington, M.S. Sol-Gel derived antireflective coatings for silicon. *Solar Energy Mater.* **1981**, *5*, 159–172. [CrossRef]
15. Richards, B.S. Single-Material TiO_2 double-layer antireflection coatings. *Solar Energy Mater. Solar Cells* **2003**, *79*, 369–390. [CrossRef]
16. Hashimoto, K.; Irie, H.; Fujishima, A. TiO_2 photocathalysis: A historical overview and future prospects. *Jpn. J. Appl. Phys.* **2005**, *44*, 8269–8285. [CrossRef]
17. Vitanov, P.; Loozen, X.; Harizanova, A.; Ivanova, T.; Beaucarne, G. A study of sol-gel deposited Al_2O_3 films as passivating coatings for solar cells application. In Proceedings of the 23rd European Photovoltaic Solar Energy Conference and Exhibition, Valencia, Spain, 1–5 September 2008; pp. 1596–1599.
18. Liang, Z.; Chen, D.; Feng, C.; Cai, J.; Shen, H. Crystalline silicon surface passivation by the negative charge dielectric film. *Phys. Procedia* **2011**, *18*, 51–55. [CrossRef]
19. Wang, M.T.; Wang, T.H.; Lee, J.Y. Electrical conduction mechanism in high-dielectric-constant ZrO_2 thin films. *Microelectron. Reliab.* **2005**, *45*, 969–972. [CrossRef]
20. Born, M.; Wolf, E. *Principle of Optics*, 7th ed.; Cambridge University Press: Cambridge, UK, 1999; p. 67.
21. Kern, W.; Puotinen, D.A. Cleaning solutions based on hydrogen peroxide for use in silicon semiconductor technology. *RCA Rev.* **1970**, *31*, 187–206.
22. *Handbook of Silicon Wafer Cleaning Technology*, 2nd ed.; Reinhardt, K., Kern, W., Eds.; William Andrew Publishing: New York, NY, USA, 2008.
23. Koch, W. Properties and uses of ethylcellulose. *Ind. Eng. Chem.* **1937**, *29*, 687–690. [CrossRef]
24. Kobiyama, M. *Basic Theory of Thin Film Optics*; Optronics Co. Ltd.: Tokyo, Japan, 2003; ISBN-10:4-900-47496-7, ISBN-13:978-4900474963. (In Japanese)